MAUSAM, **74**, 3 (July, 2023), 741-760

MAUSAM

DOI : https://doi.org/10.54302/mausam.v74i3.2976
Homepage: https://mausamjournal.imd.gov.in/index.php/MAUSAM

UDC No. 551.584.5 : 551.5

Determining the influence of meteorological parameters on outdoor thermal comfort using ANFIS and ANN

RISHIKA SHAH, R. K. PANDIT* and M. K. GAUR**

PhD Candidate, Madhav Institute of Technology and Science, Gwalior – 474 005, India

**Director, Madhav Institute of Technology and Science, Gwalior – 474 005, India*

***Professor, Madhav Institute of Technology and Science, Gwalior – 474 005, India*

(*Received 27 September 2021, Accepted 27 October 2022*)

e mail : shahrishika24@gmail.com

सार — इस अध्ययन का उद्देश्य इनपुट प्राचल के रूप में मौसम संबंधी प्राचलों का उपयोग करके बाहरी ऊष्मीय सुविधा का पूर्वानुमान करने के लिए कृत्रिम तंत्रिका नेट वर्क विकसित करना है। सारभौमिक ऊष्मीय जलवायु सूचकांक (यूटीसीआई) का उपयोग लक्ष्य प्राचल के रूप में किया जाता है। इस उद्देश्य के लिए, भारत के ग्वालियर शहर की चार मुख्य शहरी सड़कों से 5088 घंटे के क्षेत्र निगरानी डेटा पर विचार किया गया। सबसे पहले, मौसम संबंधी प्राचलों के बीच रैखिक संबंध निर्धारित किया गया। औसत विकिरण तापमान का भूमंडलीय तापमान और सतह तापमान के साथ उच्च सहसंबंध होना था। दूसरा, UTCI पर उनके प्रभाव के क्रम में मौसम संबंधी प्राचलों को श्रेणीबद्ध करने के लिए एडेप्टिव न्यूरो फ़ज़ी इनफेरेंस सिस्टम (ANFIS) का उपयोग किया गया। हवा के तापमान का सबसे अधिक प्रभाव पाया गया। तीसरा, एएनएन मॉडल इनपुट परत में एकमात्र मौसम प्राचल के रूप में हवा के तापमान के साथ यूटीसीआई का पूर्वानुमान करने के लिए विकसित किए गए हैं। सभी चार सड़कों के लिए विकसित एएनएन मॉडल ग्रीष्म (R2 = 0.852, 0.986, 0.962, 0.955) और शीत ऋतु (R2 = 0.976, 0.870, 0.941, 0.950) दोनों के लिए उल्लेखनीय पूर्वानुमान देने की क्षमता दिखाते हैं। इसके अतिरिक्त, विकसित मॉडलों का सफलता सूचकांक ग्रीष्म ऋतु में 0.73 - 1, 0.88 - 1, 0.86 - 1, 0.87 - 1 और शीत ऋतु में 0.78 - 0.99, 0.61 - 0.98, 0.55 - 0.98, 0.87 - 0.99 की सीमा में पाया गया है। यह अध्ययन स्मार्ट सिटी की अवधारणा के अनुसार भविष्य के शहरी डिजाइन में योगदान देता है,जब मशीन से सीखने के दृष्टिकोण का उपयोग करके अन्य माइक्रॉक्लाइमैटिक प्राचलों को रिकॉर्ड करना मुश्किल होता है तब स्थापित करके हवा के तापमान के उपयोग द्वारा बाहरी ऊष्मीय सुविधा का आसानी से अनुमान लगाया जा सकता है।

ABSTRACT. The study aims to develop artificial neural networks to predict outdoor thermal comfort using meteorological parameters as input parameters. Universal Thermal Climate Index (UTCI) is used as the target parameter. For this purpose, 5088 hours of field monitoring data were considered from four representative urban streets of Gwalior city, India. First, linear association was determined between meteorological parameters. Mean radiant temperature was to be in high correlation with globe temperature and surface temperature. Second, the Adaptive Neuro Fuzzy Inference System (ANFIS) was used to rank the meteorological parameters in order of their impact on UTCI. The air temperature was found to be having the strongest influence. Third, ANN models are developed to predict UTCI with air temperature as the only meteorological parameter in the input layer. The developed ANN models for all four streets show remarkable predictive ability for both the summer (R2 = 0.852, 0.986, 0.962, 0.955) and the winter season (R2 = 0.976, 0.870, 0.941, 0.950). Additionally, the success index of the developed models is found to be in range 0.73 – 1, 0.88 – 1, 0.86 – 1, 0.87 – 1 for the summer season and 0.78 – 0.99, 0.61 – 0.98, 0.55 – 0.98, 0.87 – 0.99 for the winter season. The study contributes to the smart city initiatives for future urban design by establishing that outdoor thermal comfort can be easily predicted using air temperature when other microclimatic parameters are difficult to record using a machine learning approach.

Key words – Smart city, ANFIS, ANN, Air Temperature, Outdoor Thermal Comfort.

1. Introduction

The global built environment is under expansion at an unmatched scale but has brought global challenges. Climate change is one of the direct consequences of the high-speed urbanization the world is facing. The international panels are estimating that the 230 billion square meters of built-up floor area will be added to the

TABLE 1

Recent studies on outdoor thermal comfort in India

S.No.	Location	Thermal Comfort Index	Study Area Typology	Period of study	Research Method	Climate
1.	Bhopal	PET	Urban Parks, Markets	March 12-15 and April 17-19, 2016 1230 pm to 400 pm	Subjective assessment Statistics	Composite
2.	Chennai	PET	Mixed-Use Neighborhood	15 February and 15 March, 2018 for the winter readings and 30 April - 30 May, 2018 for summer readings 0000 and 0430 h'	ENVI-met simulations	Warm and Humid
3.	Chennai	PET	Streets	0710 am, 1045 am, 0400 pm and 0615	RayMan	Warm and Humid
4.	Chennai	PET	A Mixed-Use Residential Neighborhood	May 15 to June 15, 2018	ENVI-met simulations	Warm and Humid
5.	New Delhi	PET	Open-Air Markets	9 - 12th (June, 2018) between 1100-1800 h	RayMan	Composite
6.	English Bazar Municipality	DI, PET, PMV	Neighborhood	Year of 2010 and 2016	RayMan	Warm and Humid
7.	Kolkata	PET	Micro Entrepreneur Communities		RayMan Pro	Warm and Humid
8.	Mumbai	Air temperature	Informal Settlement	August 10, 2016 through August 23, 2016	DesignBuilder v4.7 and EnergyPlus v8.3.	Warm and Humid
9.	Mumbai	Surface temperature, Air temperature	Recreational Open Spaces	0900 h to 2100 h, *i.e*., for 12 h for 24th March, 2017	ENVI-met	Warm and Humid
10.	Nagpur	DI	City	(Morning 9 am to evening 6 pm), the transition period from office, market and home (evening 6 pm to 10 pm) and nocturnal hours (10 pm to 6 am)	One-way ANOVA	Hot and Dry
11.	New Delhi	PET & UTCI	Urban Square	5 days (June 10-14, 2017) between 1100 and 1800 h	RayMan	Composite
12.	Central-NCR (CNCR)	UHI	City	1-15 May 2012	MODIS nocturnal LST	Composite
13.	Noida	UTFVI	City	2011 - 2019		Composite
14.	Sonepat	WBGT, UTCI, PET	City	January 2010 to December 2019	Microsoft Excel 2016 and SPSS 23Pearson product moment correlation	Composite
15.	Sriniketan-Santiniketan Planning Area (SSPA)	LCZ	Neighbourhood		ANOVA and Krushkal-Walls test	Warm and Humid

*The climate zones are specified in reference to Climate Zone map of India, National Building Code 2016 (Bureau of Indian Standards, 2016)

already existing one by the year 2060 (United Nations, 2017). According to the World Bank, the global urban population has increased from 28.3% to 50% since 1950. Similarly, India's urban population has increased from 17.35% to 31.2% since 1950, showing an annual urban population growth rate of 3.35% (Census of India 2011).

The recent trends on sustainable development and climate change have drawn significant attention to compelling actions and research for solutions. Sustainable Development Goals (SDGs) 7, 11, 12 & 13 of the 2030 Agenda for Sustainable Development aim to devote to affordable & clean energy, sustainable cities

&communities, responsible consumption & production, and climate action, respectively. One of the key focuses of Sustainable Development Goal (SDG) 11 and 13 for SDG Agenda 2030 are to take climate action toward creating sustainable cities (United Nations, 2017). Following the global warming trends, surface temperatures in India have increased by approximately 0.055 K per decade during the years 1860 to 2005. Greenhouse Gases (GHG) and land use planning are the crucial factors contributing to these global warming trends during the 20th century (Basha *et al*., 2017). The increase in temperatures will seriously impact the health of urban residents. Physical well-being is parallel to outdoor thermal comfort, directly associated with urban microclimate influenced by urban physics. In this regard, Urban Heat Island (UHI), Surface Urban Heat Island (SUHI) and Urban Canopy Layer (UCL) are the most studied (ASHRAE & American National Standards Institute, 2004).

Outdoor thermal comfort in varied urban microclimates of cities is an essential parameter in urban design (Silva, 2017). A growing interest is observed in climate change and global warming trends analysis for better urban design in India. Ali *et al*. performed a study in urban parks, market, and lakefront in Bhopal to understand thermal perception in the summer season. The study focussed on the effects of vegetation on outdoor thermal comfort through subjective and ordinal logistic regression and Rayman software.The study established that urban parks were cooler than markets and lakefronts and statedthat globe temperature has a high influence on thermal perception, however, the data was collected from 1230 pm to 0400 pm from March 12-15 and April 17-19, 2016 (Binte and Patnaik, 2017). Similarly, the urban heat island effect for a neighborhood in Chennai using PET for assessment and observed that the hot pockets are found in areas of low vegetation and low built density and high Sky View Factor (SVF). The simulated results were computed through ENVI-met software. (Amirtham, 2007; Horrison *et al*., 2021; Horrison and Amirtham, 2016) Manavvi and Rajasekar conducted studies on open-air markets of New Delhi for four representative summer days (9 - 12th June, 2018) between 1100-1800 hoursand thermal comfort observations based onthe relationship between surface temperatures, PET and albedo (Manavvi and Rajasekar, 2021). The authors performed similar study in religious urban square in New Delhi for 5 summer days from 1100 and 1800 h and found that Sky View Factor (SVF) influences mean radiant temperature and PET(Manavvi and Rajasekar, 2019).

Ziaul and Pal used satellite data to analyse Discomfort Index (DI) and PET for English Bazar Municipality, West Bengal. The authors compared seasonal thermal discomfortability of 2010 and 2016 and deduced that finer spatial resolution produce better results (Ziaul and Pal, 2019). Banerjee *et al*. studied outdoor thermal comfort in three micro-entrepreneur communities in Kolkata, India, through TSV and PET using field measurement and surveys. The study was carried out for November 2018 - February 2019 and in June 2019 from 1100 hours to 1700 hours, which concluded that PET is a better indicator of thermal comfort than the air temperature. Availability of shade was an important factor in influencing the duration of stay in different community areas (Banerjee *et al*., 2020). Nutkiewicz *et al*. studied the impact of early-stage design decisions in redevelopment projects through the case study of an urban slum in Mumbai. The authors simulated the area by employing an energy modeling framework and stated that if the current designs are replicated in vertical form, the impact on outdoor thermal comfort could be worse; hence simulation of design in an early stage is necessary (Nutkiewicz *et al*., 2018).

Mehrotra *et al*. assessed the impact of urban form and land surface treatment on the thermal profile of recreational open spaces. The analysis was performed using the ENVI met model. The authors concluded that surface temperature significantly influencesair temperature in open urban spaces (Mehrotra *et al*., 2021). Kotharkar *et al*. studied outdoor thermal comfort in Nagpur through LCZ (Local Climate Zone) Classification method and one-way ANOVA technique. The authors deduced that different areas in the city show variance in thermal comfort due to different built form configurations, building and street geometry (Kotharkar *et al*., 2019). Mohan *et al*. attempted to quantify the change in urbansprawl evolution from 1972-2014 in CNCR (Central National Capital Region) and studied the impact of thermal comfort. The study showed an increase in extremely thermally uncomfortable hours from an average of 10 hours to 13 hours a day based on Robba Index results (Mohan *et al*., 2020). Using the UTFVI (Urban Thermal Field Variance Index), Sharma *et al*. evaluated the thermal comfort levels of Noida cityand highlighted an increase of 6.42 °C between 2011 to 2019 (Sharma *et al*., 2021). Kumar and Sharma assessed the monthly heat stress risk to the the well being of residents in Sonepat. The authors used three thermal comfort indices namely - WBGT (Wet Bulb Globe Temperature), UTCI (Universal Thermal Climate Index), PET (Physiological Equivalent Temperature). Using PET, Das *et al*., evaluated neighborhood in Sriniketan-Santiniketan Planning Area (SSPA) through LCZ approach, concluding that low rise compact built forms are warmer for warm humid climatic zone.

Recently, artificial neural networks (ANN) have been used for the prediction of outdoor thermal comfort

due to their advantage in solving nonlinear problems (Lee *et al*., 2016). In the past, ANN for forecasting outdoor thermal comfort has been applied for urban squares, urban parks, built forms, and streets. However, these studies establish the efficiency of ANN models to predict outdoor thermal comfort for urban parks and squares. Essentially two centralbuilt environment typologies have been found in literature as study areas in this research topic - urban built form and street canyons. Dombayci *et al*., proved that ANN could be a dependable tool in predicting temperature by predicting daily mean temperature for thermal analysis in Turkey (Dombaycı and Golcu, 2009). Gobakis *et al.*, compared Elman, feedforward, and cascade neural networks urban heat intensity for Athens establishing that feed-forward neural network predicted with an accuracy of 90% (Gobakis *et al*., 2011). Vouterakos *et al*. predicted discomfort index and found that ANN models can predict Discomfort Index (DI) values on days when discomfort has surpassed disastrous levels (Vouterakos *et al*., 2012). Kamoustsis and Chronopoulos (Chronopoulos *et al*., 2012) performed a comparative study of thermohygometric index for Greek mountainous regions using only relative humidity and air temperature. Moustris *et al*., predicted human thermal comfort discomfort levels for the Greek island and one-day prediction of PET for different periods (Moustris *et al*., 2013). Papantoniou and Kolokotsa predicted outdoor air temperature using neural network models, taking four European cities as case studies (Papantoniou and Kolokotsa, 2015). Ketterer mapped PET for urban cities in Stuttgart, Germany, comparing ANN and SMLR using backpropagation training (Ketterer and Matzarakis, 2016). Lee predicted heat island intensity for Seoul using green area, water area, building area, road area and microclimatic factors (Lee *et al*., 2016). Different authors forecasted PET in Serbian urban parks - Vučković *et al*., applied neuro-fuzzy with accuracy of 92% using global radiation, vapour pressure, wind speed as input parameters (Vučković *et al*., 2019) and Protic *et al*., used 1 minute sampling for one month using global radiation, vapour pressure and wind speed (Ivana S. Bogdanovic *et al*., 2016). Bozorgi *et al*., used a middle layer feedforward neural network to estimate land surface temperatures in urbanized landscapes (Bozorgi and Nejadkoorki, 2018). Moustris developed ANN models to study PET using climatic data from a standard meteorological station in Athens for 4 sites: an urban square, urban street, urban courtyard, and urban gallery of a neighbourhood with a predictive ability of 96% (Moustris *et al*., 2018). Chan *et al*., developed an artificial neural network for predicting outdoor thermal comfort in community parks in urban Hong Kong. The authors predicted PMV to study the thermal sensation, but the environmental simulation was excluded due to complex quantification (Chan and Chau, 2019). Weerasuriyaa *et al*., optimized lift-up buildings to maximize pedestrian thermal comfort using wind speed as a primary parameter to predict UTCI through a genetic algorithm, computational fluid dynamics simulation, and artificial neural network (Weerasuriya *et al*., 2020).

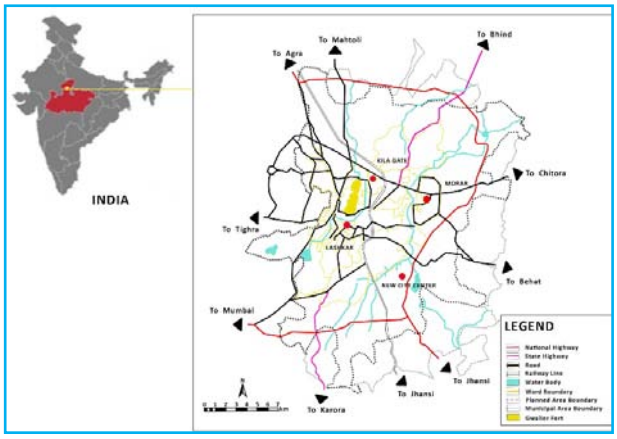

Fig. 1. Location of Gwalior in India

It is evident from the existing literature that the studies performed on outdoor thermal comfort analysis in India either consider limited amount of time period when using software with less computaional time (Ray Man), or only analysing few days when software in use has high simulation run time (ENVI-met). When studies over a period of years are conducted, the real time data collection and accessibility of remote sensing maps sometimes become difficult. Hence, in this study an attempt to study outdoor thermal comfort using a different methodology - artificial neural network is adopted as it is proved to handel large number of data in less operational time. In studies regarding outdoor thermal comfort and ANN, it is seen that studies on urban streets have only shown data concerning one particular season in the year or only diurnal data is evaluated (Moustris, Nastos and Paliatsos, 2013; Ketterer and Matzarakis, 2016; Banerjee and Chattopadhyay, 2020). After urban parks and squares, streets are the open spaces that are used by city dwellers on a large scale. Microclimates of urban streets have a direct influence on outdoor and indoor thermal comfort of the built environment and corresponding energy demand (Silva, 2021). Therefore, in this study, artificial neural networks models are developed to predict the outdoor thermal comfort of four different street canyons that can be seen as representative of the historical city of Gwalior, India. The focus is to develop and apply a neural network where air temperature can be utilized only as a meteorological input parameter to predict outdoor thermal comfort. Additionally, the correlation of heat with built environmental parameters are also discussed to provide insights for city development policies.

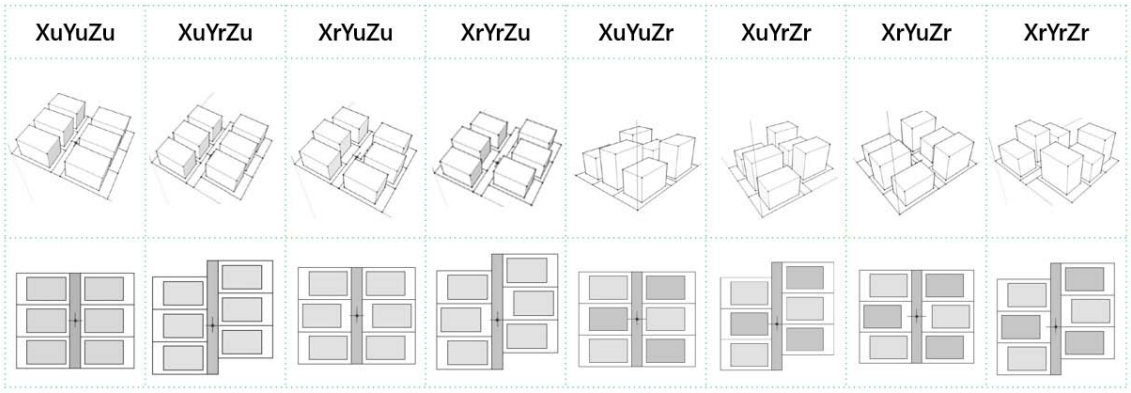

Fig. 2. Generic categories of built forms

1.1. *Study area*

The study site is located in the historic city of Gwalior located at 26.2183° N, 78.1828° E (Fig. 1), the city is currently listed as a potential Smart City under Smart Cities Mission (Ministry of Housing and Urban Affairs, 2015). The importance of Gwalior city as a historic city can be observed from its inclusion as one of the pilot cities for the Historic Urban Landscape programme and survey under UNESCO New Delhi, directing heritage based urban development (UNESCO New Delhi, 2021).

The city has majorly evolved since the 8thcentury into four representative zones - Kila Gate zone, Lashkar zone, Morar Zone and New City Centre zone. Kila Gate zone is the first settlement area at the base of Gwalior fort, followed by Lashkar area which was established by the Mughals in 1810, Morar area was instituted as a British cantonment area, and in the past few decades, the city has seen modern construction in the New City Centre area. Hence, out of these four zones two are historic in context (Kila Gate & Lashkar) and the other two are modern (Morar & New City Center). The streets were selected to represent different neighbourhoods - historic and modern, and of different urban physics parameters. These parameters represent street geometry which includes street orientation, height width ratio and built form configuration. The built forms correspond to uniform or random layouts, where "u" represents uniform layout and "r" represent random layout (Cheng *et al.*, 2006). Each built form can be denoted in context of *X* axis, *Y* axis and Z axis. Hence, the eight generic categories of built forms are: XuYuZu, XuYrZu, XrYuZu, XrYrZu, XuYuZr, XuYrZr, XrYuZr and XrYrZr (Fig. 2). The street geometries of the study area is tabulated in Table 2. For ease of understanding, these streets are named after their respective zones, *i.e.*, Kila Gate (KG), Lashkar (LAS), Morar (MOR) and New City Centre (NCC).

TABLE 2

Street Geometry of the selected case studies

Location	Street orientation	H/W	Built Form
Kila Gate (KG)	NW-SE	3.3	$X_rY_rZ_r$
Lashkar (LAS)	N-S	4.08	$X_rY_rZ_u$
Morar (MOR)	EW	1.6	$X_uY_uZ_r$
New City Center (NCC)	SW-NE	0.9	$X_uY_uZ_u$

Also, ease of instrument set up and monitoring of data from these streets worked as contributing faction in choice of these streets. The selected four street canyons are graphically shown in Fig. 3.

1.2. *Climate profile*

The study area observes extreme summers and extreme winters featuring composite climatic conditions according to the National Building Code of India 2016 (Bureau of Indian Standards, 2016). The high temperatures are noticed beginning from mid to late March, rising in May and June between 33°C-35°C. The low temperatures are observed from late October and found lowest in January with an average temperature of around 5°C-6°C. As per the universal Köppen Climate Classification, the study site is classified under group C in the subgroup Cwa (dry winter humid subtropical climate) bordering with the classification BSh (dry semi-arid climate with low latitude).

1.3. *UTCI*

To assess the heat stress in the streets, the Universal Thermal Climate Index (UTCI) was chosen for this study. UTCI was selected due to its validation as a heat stress

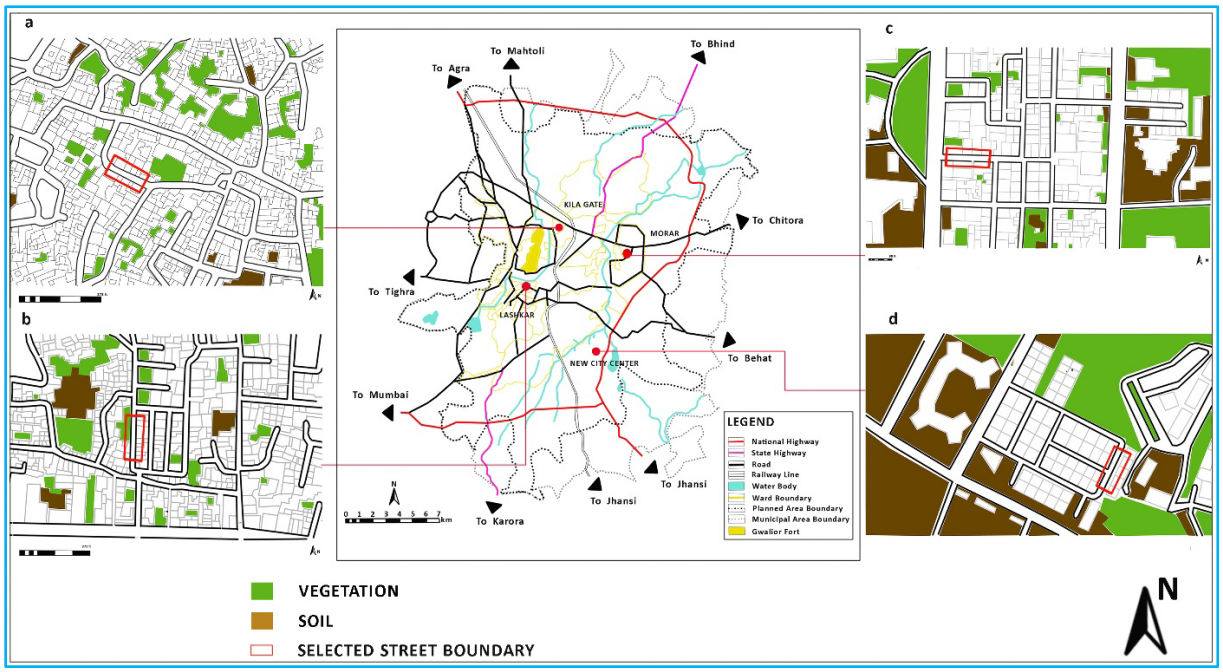

Fig. 3. Description of study area

TABLE 3

Thermal stress range for UTCI

Thermal Stress Class	UTCI Index Range (°C)
Extreme heat stress	above +46
Very strong heat stress	+38 to +46
Strong heat stress	+32 to +38
Moderate heat stress	+26 to +32
Slight heat stress	
No thermal stress	+9 to +26
Slight cold stress	0 to +9
Moderate cold stress	-13 to 0
Strong cold stress	-27 to -13
Very strong cold stress	-40 to -27
Extreme cold stress	below -40

index according to the existing literature and its uncomplicated interpretation by urban designers and architects due to its unit of measurement in degree Celsius (°C). UTCI is expressed as the ambient air temperature of the thermal environment which is referred to. This thermal index generates the same stress index value in comparison with the reference human being's response to the existing environs. Derived from the advanced multi-node thermoregulatory model, UTCI is universal due to its established efficacy in evaluating thermal environments of all climatic zones (UTCI, 2021). The thermal stress range for UTCI is shown in Table 3. BioKlima 2.6 was used to determine the hourly values of UTCI (Krzysztof Błażejczyk, 2021).

2. Methodology

2.1. *Methods*

The study is based on recording and analysing meteorological variables for analysis of the Universal Thermal Climate Index, therefore, first the correlation between the recorded parameters was analysed. Pearson correlation coefficient was used to determine the linear association between the input parameters in order to avoid redundancies and over-fitting in the ANFIS and ANN models. This correlation was determined by using:

$$r = \frac{\sum (x_i - \underline{x})(y_i - \underline{y})}{\sqrt{\sum (x_i - \underline{x})^2 \sum (y_i - \underline{y})^2}} \quad (1)$$

Following this, ranking of meteorological parameters is conducted using the Adaptive Neuro Fuzzy Inference (ANFIS) system. The implementation of ANFIS models is based on input/output data pairs. The analysis is performed using the Neuro Fuzzy Designer application. The model was run in MATLAB 2019 (a) for

TABLE 4

Details of instruments used in this study

Name of the instrument	Parameter measured	Accuracy	Range	Standard uncertainty
Elitech RC-4HC	Air temperature	±0.6 °C	-30° - 60°C	0.346 °C
Elitech RC-4HC	Relative humidity	±3 %	0- 99 %	1.732 %
Lutron AM-4237 SD Anemometer	Wind speed	±0.05 m/s	0.1 – 25 m/s	0.028 m/s

regression of data pairs. As part of this process, training error output and testing error output are derived. The variable ranking is noted on the basis of training error. 50% of testing data is used to control the fitting of training data. Normalization of data is performed using a fuzzify function during the training process, thus, making the neuro fuzzy system an appropriate choice for ranking of meteorological parameters (Vouterakos *et al*., 2012).

Based on the ranking of meteorological parameters, artificial neural network models are developed to predict selected outdoor thermal comfort index, *i.e*., UTCI. Multiple Layer Perceptron Models are observed to have high efficacy rates in the available literature, hence multiple layer perceptron model is used in this work(Milojevic-Dupont and Creutzig, 2021). These models are developed using back propagation training algorithms to predict UTCI. The structure of the basic artificial neural network model consists of neurons that are organized in layers, which start with an input layer followed by a hidden layer and final output layer. The input layer distributes the input signals to the first hidden layer, which transmits the signal to each neuron of the next hidden layer, corresponding to a weight factor. In this way, each neuron gets processed through the input and hidden layers in addition to the activation function and finally, the outcome reaches the output layer. The input layer contains input variables, the target variable is represented by the output layer and the number of hidden layers is determined using Eqn. 2 (Chan and Chau, 2019). The actual outcome is then compared for its closeness with the desired outcome, which determines the accuracy of the ANN model.

$$2\times\sqrt{N_i}+N_0\le N_h\le 2\times N_i+1 \quad (2)$$

Once the ANN models are developed their validation is performed by evaluating TPR, FAR and SI of the developed models and through the coefficient of correlation between calculated and predicted values of UTCI using Eqns. 3 - 5 (Vouterakos *et al*., 2012).

$$\mathrm{TRP}=\frac{X}{X+Y} \quad (3)$$

$$\mathrm{FAR}=\frac{Z}{Z+X} \quad (4)$$

$$\mathrm{SI}=\frac{X+W}{X+Y+Z+W} \quad (5)$$

where, *X* denotes the number of occurrences where the thermal comfort values were calculated and predicted in the same thermal stress class, *Y* denotes the number of occurrences where the calculated thermal comfort values fit in a specific class but the predicted value fit in some other class, *Z* denotes the number of occurrences where the predicted thermal comfort values fit in a specific class, but calculated value fit in some other class and W denotes the rest of the cases.

2.2. *Data collection*

The functional process of ANN depends upon the huge historical database for training, the choice of input parameters and training algorithms. Field measurements were carried out for seven months. This period was divided into the winter and the summer season. The winter season is represented by months - December 2020, January and February 2021 and the summer season by - March, April, May and June 2021. Continuous hourly data of air temperature, wind speed and relative humidity for all four streets were recorded simultaneously. The recording of microclimatic data was carried out using Lutron AM 4237 SD Data Logger Anemometer for wind speed and Elitech RC - 4HC Data Logger with an inbuilt sensor for relative humidity and a probe for air temperature. Details of the instruments are shown in Table 4. A total number of 5088 hours of field monitoring data was collected. For ANFIS model 50% of the recorded data was used as training data set and for ANN models 70% of the recorded data as training data set.

TABLE 5

Correlation between input variables for summer and winter from the Kila Gate data set

	Summer						Winter					
	Ta	RH	WS	Ts	Tmrt	Tg	Ta	RH	WS	Ts	Tmrt	Tg
Ta	**1**						**1**					
RH	0.34	1					-0.705	1				
WS	**0.004**	**0.002**	**1**				**0.023**	**-0.161**	**1**			
Ts	0.42	0.09	0.02	1			0.967	-0.716	0.336	1		
Tmrt	**0.32**	**0.06**	**0.02**	**0.95**	**1**		**0.652**	**- 0.534**	**0.312**	**0.785**	**1**	
Tg	0.20	0.03	0.02	0.94	0.93	1	0.570	-0.510	0.142	0.723	0.939	1

TABLE 6

Correlation between input variables for summer and winter from the Lashkar data set

	Summer						Winter					
	Ta	RH	WS	Ts	Tmrt	Tg	Ta	RH	WS	Ts	Tmrt	Tg
Ta	**1**						**1**					
RH	0.379	1					-0.599	1				
WS	**0.047**	**-0.042**	**1**				**0.065**	**-0.091**	**1**			
Ts	0.636	-0.247	0.079	1			0.702	-0.453	0.079	1		
Tmrt	**0.567**	**-0.199**	**0.081**	**0.977**	**1**		**0.400**	**-0.275**	**0.137**	**0.821**	**1**	
Tg	0.442	-0.195	0.079	0.972	0.965	1	0.286	-0.237	0.129	0.733	0.930	1

TABLE 7

Correlation between input variables for summer and winter from the Morar data set

	Summer						Winter					
	Ta	RH	WS	Ts	Tmrt	Tg	Ta	RH	WS	Ts	Tmrt	Tg
Ta	**1**						**1**					
RH	-0.511	1					-0.736	1				
WS	**0.040**	**-0.003**	**1**				**0.302**	**-0.268**	**1**			
Ts	0.670	-0.361	0.106	1			0.813	-0.683	0.311	1		
Tmrt	**0.607**	**-0.322**	**0.106**	**0.978**	**1**		**0.694**	**-0.617**	**0.315**	**0.978**	**1**	
Tg	0.465	-0.277	0.113	0.968	0.961	1	0.488	-0.507	0.296	0.900	0.959	1

TABLE 8

Correlation between input variables for summer and winter from the New City Centre data set

	Summer						Winter					
	Ta	RH	WS	Ts	Tmrt	Tg	Ta	RH	WS	Ts	Tmrt	Tg
Ta	**1**						**1**					
RH	-0.560	1					-0.804	1				
WS	**0.083**	**-0.173**	**1**				**0.077**	**-0.120**	**1**			
Ts	0.757	-0.455	0.090	1			0.837	-0.756	0.087	1		
Tmrt	**0.693**	**-0.420**	**0.121**	**0.979**	**1**		**0.721**	**-0.684**	**0.110**	**0.978**	**1**	
Tg	0.521	-0.356	0.147	0.949	0.952	1	0.471	-0.530	0.109	0.874	0.943	1

TABLE 9

Training error values for summer and winter for all four study locations

Location	Phase	Summer				Winter			
		Ta	RH	WS	Tmrt	Ta	RH	WS	Tmrt
KG	Training phase	1.67	3.85	4.72	2.14	1.99	3.97	4.32	2.32
	Testing phase	1.08	3.79	4.56	2.18	1.79	3.88	4.21	2.06
LAS	Training phase	1.64	3.46	4.05	3.54	1.74	3.12	4.09	2.25
	Testing phase	1.7	3.43	4.97	3.8	1.71	3.65	4.88	2.41
MOR	Training phase	1.72	3.93	4.73	2.95	1.46	3.03	4.76	2.19
	Testing phase	1.9	3.89	4.62	2.65	1.39	3.15	4.72	2.08
NCC	Training phase	1.5	3.07	4.89	3.94	1.83	3.66	4.58	2.63
	Testing phase	1.81	2.99	4.91	3.18	1.81	3.59	4.39	2.56

TABLE 10

Description of developed ANN Models

	Category 1	Category 2
Input parameter	Ta, RH, WS, Tmrt, Month of the year, Day of the month, Hour of the day	Ta, Month of the year, Day of the month, Hour of the day
Target parameter	UTCI	UTCI

3. Results and discussion

3.1. *Pearson correlation*

Tables 5-8 represent the correlation between input variables for summer and winter for all four streets. Very low correlation coefficients are observed from these tables between the recorded input variables. However, a high collinearity was observed between globe temperature (Tg), mean radiant temperature (Tmrt) and surface temperature (Ts). The value of high correlation coefficients are highlighted in bold in the tables. This high correlation between Tmrt, Tg and Ts may lead to overfitting and unnecessary repetitions in the developed neural network models (Vučković *et al.*, 2019). Accordingly, Tmrt is used for further analysis against Ts and Tg in ANFIS and ANN models as it is easy to calculate.

3.2. *Meteorological parameter ranking*

The recorded meteorological parameters are ranked based on training error values computed in the neuro fuzzy system. Root Mean Square Error (RMSE) is derived from the simulation. UTCI values are highly influenced by the parameters which show the lowest training RMSE value. The values are obtained by using 70% of recorded data as training data and 30% of recorded data as testing data. Theleast error is observed in air temperature on all four streets in both summer and winter. Air temperature is followed by mean radiant temperature, relative humidity and wind speed (Table 9). This establishes that air temperature has the highest impact on UTCI values in comparison to other meteorological parameters.

3.3. *UTCI prediction through ANN models*

Based on the results above, it can be inferred that air temperature is most influential in predicting the UTCI values for both the summer and the winter months. Therefore, two categories of ANN models are developed (Table 10).

As per Eqn. 1, the hidden parameters were determined. A total of 36 models were developed under Category 1 for all four sites and a total number of 45 models were developed under Category 2. The optimum predictive results are found at 12 hidden neurons for Category 1 and 6 hidden neurons for Category 2. The coefficient of correlation between calculated values of

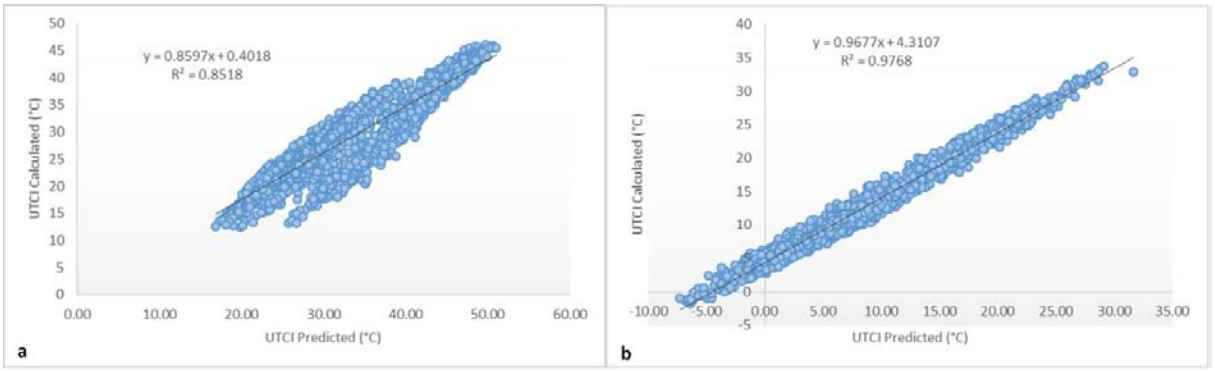

Figs. 4(a&b). Scatter plots for calculated *vs* predicted UTCI at Kila Gate (KG) - (a) Summer and (b) Winter

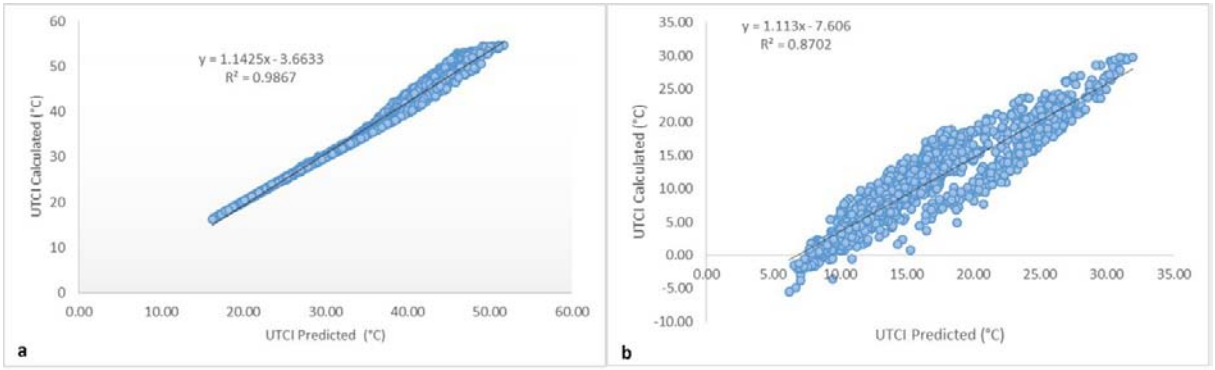

Figs. 5(a&b). Scatter plots for calculated *vs* predicted UTCI at Lashkar (LAS) - (a) Summer and (b) Winter

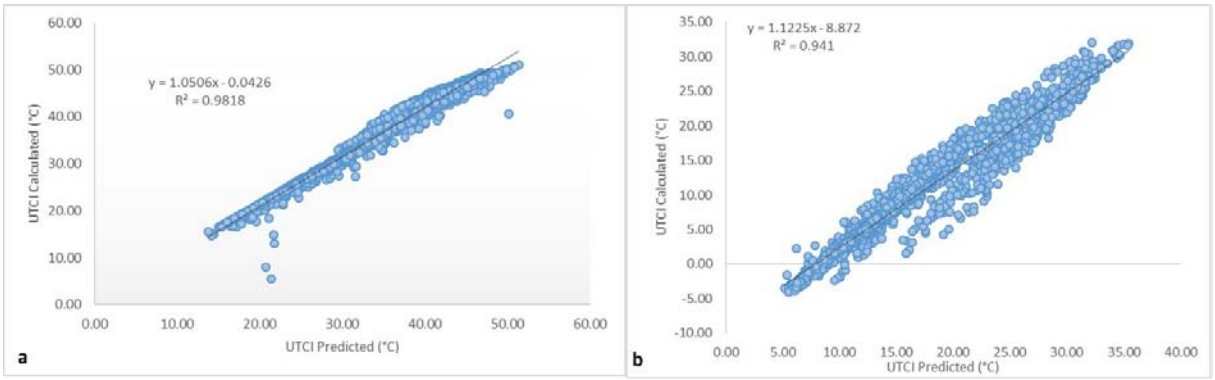

Figs. 6(a&b). Scatter plots for calculated *vs* predicted UTCI at Morar (MOR) - (a) Summer and (b) Winter

TABLE 11

Coefficient of correlation values for developed ANN models

Location	R^2 values for Summer	R^2 values for Winter
KG	0.852	0.976
LAS	0.986	0.870
MOR	0.962	0.941
NCC	0.955	0.950

UTCI from Bio Klima 2.6 and predicted values of UTCI from category1 and category 2 ANN model are analysed. It is found that the Category 1 ANN model shows high predictive ability (R^2 = 0.9 for all cases). Results for category 2 ANN models are shown in Table 11 and associated plots are shown in Fig. 4, Fig. 5, Fig. 6 and Fig. 7. Hence, it can be fairly deduced that UTCI can be predicted using the ANN model when air temperature is used as the only meteorological parameter. This also helps in reducing the usage of large numbers of instruments and complex data recording exercises.

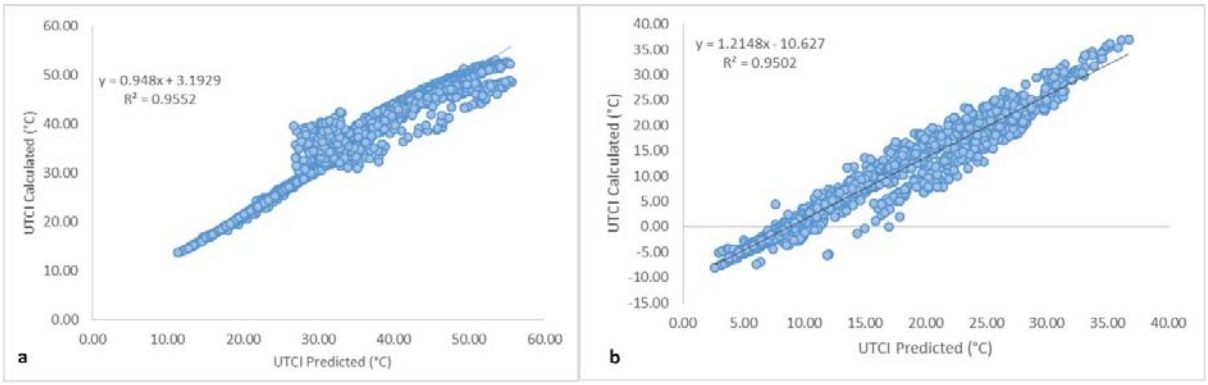

Figs. 7(a&b). Scatter plots for calculated *vs* predicted UTCI at New City Center (NCC) - (a) Summer and (b) Winter

TABLE 12

Evaluation indices of developed Category 2 ANN model for UTCI in Kila Gate for summer and winter

Thermal stress class	Index Range (°C)	X	Y	Z	W	TPR	FAR	SI
Summer								
Extreme heat stress	above +46	1	189	0	2244	0.005	0.0	0.9
Very strong heat stress	+38 to +46	213	463	189	1569	0.31	0.47	0.73
Strong heat stress	+32 to +38	154	265	375	1640	0.36	0.70	0.73
Moderate heat stress Slight heat stress	+26 to +32	403	302	270	1459	0.57	0.40	0.76
No thermal stress	+9 to +26	444	0	385	1605	1	0.46	0.84
Slight cold stress	0 to +9	0	0	0	2434	-	-	1
Moderate cold stress	-13 to 0	0	0	0	2434	-	-	1
Strong cold stress	-27 to -13	0	0	0	2434	-	-	1
Very strong cold stress	-40 to -27	0	0	0	2434	-	-	1
Extreme cold stress	below -40	0	0	0	2434	-	-	1
Winter								
Extreme heat stress	above +46	5	0	3	1995	1	0	0.99
Very strong heat stress	+38 to +46	11	3	4	1985	0.78	0.26	0.99
Strong heat stress	+32 to +38	35	12	8	1948	0.74	0.18	0.99
Moderate heat stress Slight heat stress	+26 to +32	94	24	68	1817	0.79	0.41	0.95
No thermal stress	+9 to +26	892	146	219	746	0.85	0.19	0.81
Slight cold stress	0 to +9	407	203	233	1160	0.66	0.36	0.78
Moderate cold stress	-13 to 0	24	147	0	1832	0.14	0	0.92
Strong cold stress	-27 to -13	-	-	-	-	-	-	-
Very strong cold stress	-40 to -27	-	-	-	-	-	-	-
Extreme cold stress	below -40	-	-	-	-	-	-	-

TABLE 13

Evaluation indices of developed Category 2 ANN model for UTCI in Lashkar for summer and winter

Thermal stress class	Index Range (°C)	X	Y	Z	W	TPR	FAR	SI
Summer								
Extreme heat stress	above +46	152	0	259	2517	1	0.63	0.91
Very strong heat stress	+38 to +46	515	264	68	2081	0.66	0.11	0.88
Strong heat stress	+32 to +38	446	76	12	2394	0.85	0.02	0.96
Moderate heat stress Slight heat stress	+26 to +32	740	9	37	2142	0.98	0.04	0.98
No thermal stress	+9 to +26	697	29	2	2200	0.96	0.0	0.99
Slight cold stress	0 to +9	0	0	0	2928	-	-	1
Moderate cold stress	-13 to 0	0	0	0	2928	-	-	1
Strong cold stress	-27 to -13	0	0	0	2928	-	-	1
Very strong cold stress	-40 to -27	0	0	0	2928	-	-	1
Extreme cold stress	below -40	0	0	0	2928	-	-	1
Winter								
Extreme heat stress	above +46	-	-	-	-	-	-	-
Very strong heat stress	+38 to +46	-	-	-	-	-	-	-
Strong heat stress	+32 to +38	-	-	-	-	-	-	-
Moderate heat stress Slight heat stress	+26 to +32	28	90	20	1843	0.23	0.41	0.94
No thermal stress	+9 to +26	1121	671	90	99	0.62	0.07	0.61
Slight cold stress	0 to +9	42	29	647	1263	0.59	0.93	0.65
Moderate cold stress	-13 to 0	0	0	33	1948	-	1	0.98
Strong cold stress	-27 to -13	-	-	-	-	-	-	-
Very strong cold stress	-40 to -27	-	-	-	-	-	-	-
Extreme cold stress	below -40	-	-	-	-	-	-	-

Further to determine the efficiency of the Category 2 ANN model, True Predicted Rate (TPR), False Alarm Rate (FAR) and Success Index (SI) are computed using Python Script (Appendix 1). The statistical performance values for summer and winter are noted in Table 12 for Kila Gate (KG), Table 13 for Lashkar (LAS), Table 14 for

TABLE 14

Evaluation indices of developed Category 2 ANN model for UTCI in Morarfor summer and winter

Thermal stress class	Index Range (°C)	X	Y	Z	W	TPR	FAR	SI
Summer								
Extreme heat stress	above +46	144	4	213	2443	0.97	0.59	0.922
Very strong heat stress	+38 to +46	526	215	186	1877	0.71	0.26	0.86
Strong heat stress	+32 to +38	269	184	94	2257	0.59	0.25	0.90
Moderate heat stress Slight heat stress	+26 to +32	582	94	167	1961	0.86	0.22	0.91
No thermal stress	+9 to +26	619	167	2	2016	0.78	0.00	0.94
Slight cold stress	0 to +9	0	0	2	2802	-	1	0.99
Moderate cold stress	-13 to 0	0	0	0	2804	-	-	1
Strong cold stress	-27 to -13	0	0	0	2804	-	-	1
Very strong cold stress	-40 to -27	0	0	0	2804	-	-	1
Extreme cold stress	below -40	0	0	0	2804	-	-	1
Winter								
Extreme heat stress	above +46	-	-	-	-	-	-	-
Very strong heat stress	+38 to +46	-	-	-	-	-	-	-
Strong heat stress	+32 to +38	0	26	0	1980	0	-	0.98
Moderate heat stress Slight heat stress	+26 to +32	53	239	26	1688	0.18	0.32	0.86
No thermal stress	+9 to +26	736	760	239	271	0.49	0.24	0.50
Slight cold stress	0 to +9	48	144	753	1061	0.25	0.94	0.55
Moderate cold stress	-13 to 0	0	0	151	1855	-	1	0.92
Strong cold stress	-27 to -13	-	-	-	-	-	-	-
Very strong cold stress	-40 to -27	-	-	-	-	-	-	-
Extreme cold stress	below -40	-	-	-	-	-	-	-

Morar (MOR) and Table 15 for New City Centre (NCC). These values are derived from analysis of obtained UTCI values from Bio Klima 2.6 and predicted values from category 2 ANN model. The values show high predictive ability of the Category 2 model for all four streets and both seasons.

TABLE 15

Evaluation indices of developed Category 2 ANN model for UTCI in New City Centerfor summer and winter

Thermal stress class	Index Range (°C)	X	Y	Z	W	TPR	FAR	SI
Summer								
Extreme heat stress	above +46	387	26	139	2096	0.94	0.26	0.98
Very strong heat stress	+38 to +46	393	146	203	1906	0.72	0.34	0.87
Strong heat stress	+32 to +38	254	144	164	2806	0.63	0.39	0.88
Moderate heat stress Slight heat stress	+26 to +32	434	196	109	1909	0.68	0.20	0.88
No thermal stress	+9 to +26	565	103	0	1980	0.85	0.0	0.96
Slight cold stress	0 to +9	0	0	0	2648	-	-	1
Moderate cold stress	-13 to 0	0	0	0	2648	-	-	1
Strong cold stress	-27 to -13	0	0	0	2648	-	-	1
Very strong cold stress	-40 to -27	0	0	0	2648	-	-	1
Extreme cold stress	below -40	0	0	0	2648	-	-	1
Winter								
Extreme heat stress	above +46	-	-	-	-	-	-	-
Very strong heat stress	+38 to +46	-	-	-	-	-	-	-
Strong heat stress	+32 to +38	42	60	3	3356	0.41	0.06	0.98
Moderate heat stress Slight heat stress	+26 to +32	170	107	59	3125	0.61	0.25	0.95
No thermal stress	+9 to +26	1053	264	155	1989	0.80	0.12	0.87
Slight cold stress	0 to +9	264	67	260	2870	0.79	0.49	0.90
Moderate cold stress	-13 to 0	0	0	22	3439	-	1	0.99
Strong cold stress	-27 to -13	-	-	-	-	-	-	-
Very strong cold stress	-40 to -27	-	-	-	-	-	-	-
Extreme cold stress	below -40	-	-	-	-	-	-	-

3.4. *Correlation of heat with built environment*

Figs. 8 (a-d) and 9 (a-d) shows the variations of outdoor thermal comfort, air temperature, surface temperature and mean radiant temperature in all four streets showing different height to width ratio, orientation, and built form, using the predicted thermal comfort values and recorded meteorological parameters for winter and

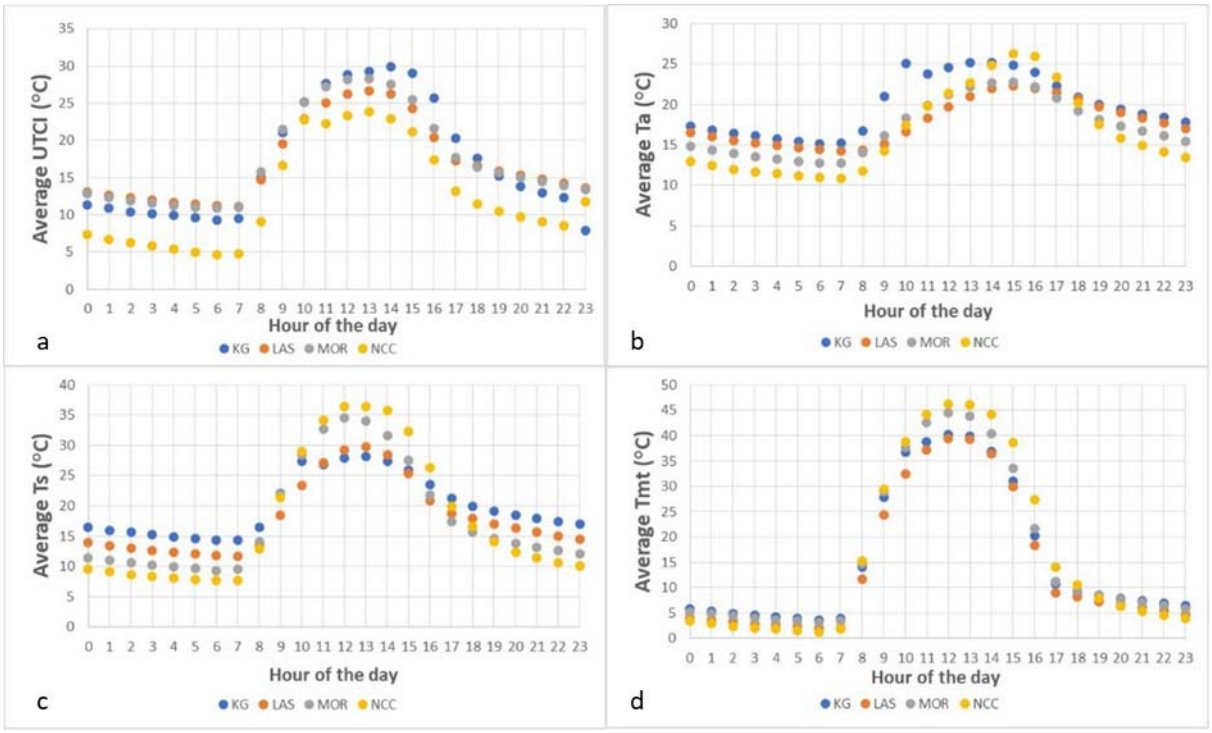

Figs. 8(a-d). Variations of (a) Average UTCI, (b) Average air temperature Ta, (c) Average surface temperature Ts and (d) Average mean radiant temperature (Tmrt) during winters

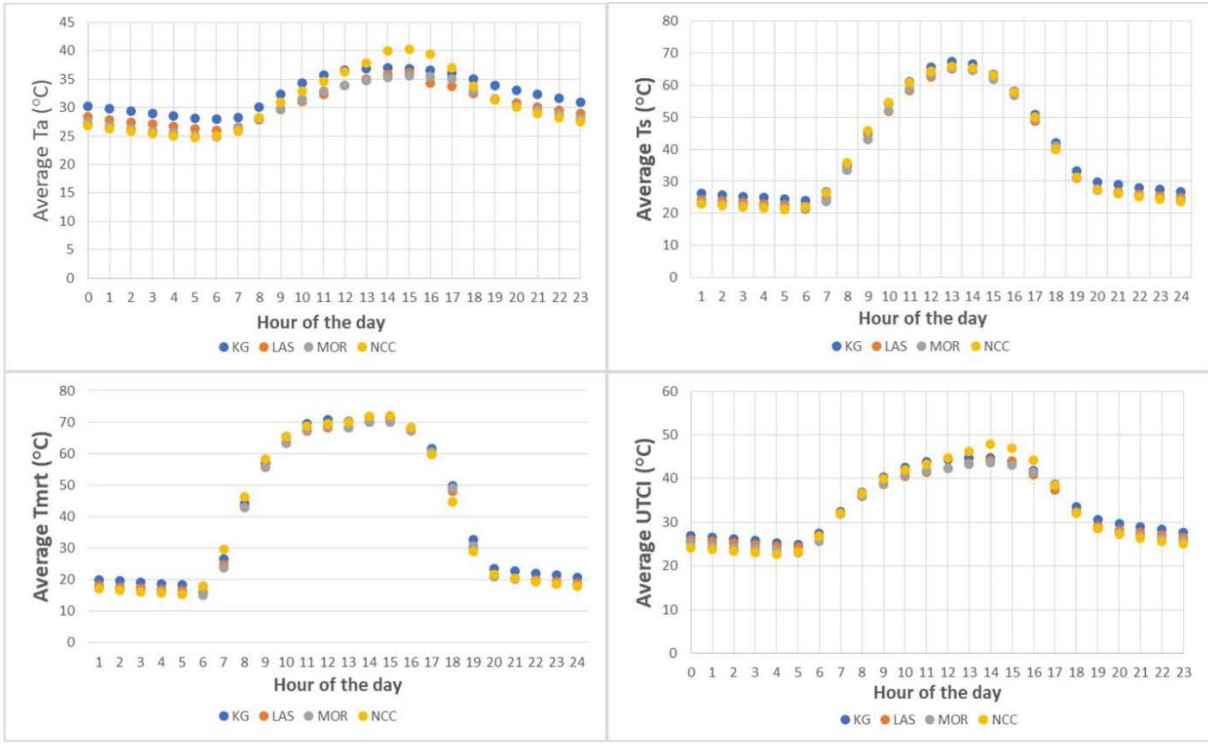

Figs. 9(a-d). Variations of (a) Average air temperature Ta, (b) Average surface temperature Ts, (c) Average mean radiant temperature (Tmrt) and (d) Average UTCI during summers

	UTCI				Ta				Ts				Tmrt			
Hour	H/W = 3.3	H/W =4.08	H/W =1.6	H/W =0.9	H/W = 3.3	H/W =4.08	H/W =1.6	H/W =0.9	H/W = 3.3	H/W =4.08	H/W =1.6	H/W =0.9	H/W = 3.3	H/W =4.08	H/W =1.6	H/W =0.9
0	11.296	13.106	12.831	7.362	17.357	16.505	14.861	12.985	16.473	13.928	11.385	9.564	5.793	4.116	5.225	3.376
1	10.858	12.681	12.288	6.727	16.827	16.022	14.399	12.520	15.956	13.454	11.024	9.113	5.285	3.649	4.795	2.899
2	10.401	12.279	11.912	6.284	16.476	15.583	13.944	12.005	15.610	13.016	10.552	8.589	4.925	3.202	4.308	2.356
3	10.104	11.957	11.585	5.833	16.121	15.214	13.571	11.692	15.258	12.661	10.163	8.293	4.568	2.839	3.908	2.030
4	9.888	11.712	11.233	5.386	15.769	14.952	13.267	11.449	14.908	12.393	9.937	8.035	4.219	2.569	3.633	1.765
5	9.656	11.446	11.062	4.974	15.439	14.645	13.013	11.196	14.581	12.094	9.683	7.790	3.904	2.272	3.363	1.497
6	9.243	11.231	10.904	4.651	15.170	14.406	12.773	10.937	14.318	11.855	9.333	7.625	3.645	2.023	3.052	1.273
7	9.548	11.134	11.016	4.779	15.251	14.211	12.770	10.861	14.400	11.660	9.483	7.701	3.929	2.037	3.401	1.808
8	15.019	14.707	15.729	9.110	16.695	14.337	14.033	11.748	16.429	13.551	14.071	12.890	14.073	11.728	14.723	15.250
9	21.078	19.563	21.508	16.598	20.982	15.181	16.136	14.292	22.075	18.505	21.905	21.396	27.883	24.398	28.888	29.477
10	25.157	22.878	25.175	22.817	25.070	16.634	18.321	17.415	27.321	23.342	28.481	29.026	36.781	32.486	37.760	38.850
11	27.654	25.050	27.184	22.209	23.746	18.302	19.948	19.822	26.819	27.106	32.686	34.157	38.762	37.266	42.587	44.167
12	28.822	26.216	28.188	23.344	24.536	19.723	21.200	21.350	27.877	29.279	34.508	36.463	40.276	39.434	44.489	46.319
13	29.200	26.637	28.308	23.824	25.189	21.000	22.144	22.706	28.235	29.733	34.086	36.443	39.879	39.252	43.854	46.042
14	29.868	26.173	27.483	22.926	25.131	21.973	22.683	24.901	27.377	28.490	31.673	35.755	36.911	36.464	40.440	44.263
15	29.016	24.315	25.475	21.110	24.851	22.317	22.758	26.203	25.860	25.358	27.488	32.263	31.014	29.954	33.598	38.576
16	25.690	20.453	21.568	17.368	23.969	21.949	22.217	25.952	23.552	20.906	21.745	26.349	20.299	18.304	21.620	27.442
17	20.280	17.278	17.670	13.146	22.320	21.476	20.837	23.341	21.318	18.667	17.420	19.875	10.665	9.046	11.264	14.043
18	17.545	16.606	16.426	11.460	20.885	20.681	19.261	20.203	19.924	17.914	15.727	16.599	9.205	8.154	9.529	10.535
19	15.212	15.867	15.613	10.486	20.052	19.717	18.136	17.511	19.113	17.007	14.605	14.008	8.438	7.296	8.487	7.944
20	13.844	15.293	14.983	9.769	19.460	18.971	17.329	15.881	18.524	16.290	13.860	12.399	7.871	6.619	7.755	6.303
21	12.994	14.776	14.463	9.058	18.862	18.337	16.701	14.908	17.939	15.682	13.202	11.447	7.313	6.018	7.102	5.331
22	12.306	14.234	13.938	8.495	18.371	17.704	16.105	14.120	17.461	15.065	12.608	10.677	6.862	5.408	6.505	4.541
23	7.904	13.615	13.361	11.761	17.871	17.036	15.495	13.501	16.963	14.405	12.033	10.073	6.386	4.739	5.882	3.910

Fig. 10. Mapping of heat distribution for streets with different height width ratio in correlation with average values of Universal Thermal Climate Index, Air Temperature, Surface Temperature and Mean Radiant Temperature during winters

	UTCI				Ta				Ts				Tmrt			
Hour	H/W = 3.3	H/W =4.08	H/W =1.6	H/W =0.9	H/W = 3.3	H/W =4.08	H/W =1.6	H/W =0.9	H/W = 3.3	H/W =4.08	H/W =1.6	H/W =0.9	H/W = 3.3	H/W =4.08	H/W =1.6	H/W =0.9
0	26.996	26.070	25.173	24.175	30.284	28.332	27.378	26.784	26.179	24.311	23.437	22.957	19.983	18.123	17.311	17.030
1	26.554	25.608	24.664	23.728	29.795	27.846	26.820	26.312	25.713	23.845	22.903	22.504	19.504	17.645	16.777	16.574
2	26.178	25.296	24.245	23.342	29.410	27.447	26.326	25.852	25.338	23.460	22.436	22.047	19.126	17.273	16.311	16.104
3	25.727	24.892	23.887	22.980	28.930	27.057	25.898	25.454	24.871	23.077	22.022	21.646	18.651	16.861	15.914	15.708
4	25.329	24.541	23.561	22.601	28.538	26.627	25.523	25.009	24.484	22.655	21.649	21.230	18.240	16.433	15.524	15.278
5	24.884	24.307	23.136	23.193	28.076	26.205	25.055	24.760	24.039	22.255	21.207	21.850	17.812	16.035	15.068	17.833
6	27.408	26.860	25.646	26.788	28.032	25.977	24.883	25.008	26.683	24.716	23.725	26.557	26.464	24.648	23.804	29.625
7	32.505	31.989	31.919	32.098	28.298	26.537	26.401	25.859	35.111	33.489	33.423	35.702	44.184	42.855	42.862	46.339
8	36.862	35.952	35.926	36.642	30.051	28.001	27.800	28.295	45.036	43.218	43.063	45.873	57.053	55.639	55.559	58.222
9	40.380	38.684	38.894	39.894	32.405	29.597	29.814	30.890	54.226	51.733	51.962	54.490	65.359	63.379	63.590	65.336
10	42.628	40.461	40.879	42.037	34.286	31.109	31.563	32.937	61.160	58.398	58.804	60.746	69.554	67.299	67.649	68.660
11	43.866	41.472	41.895	43.346	35.685	32.338	32.938	34.648	65.625	62.725	63.253	64.390	70.767	68.322	68.765	69.486
12	44.297	42.400	42.395	44.688	36.547	33.829	33.957	36.271	67.411	65.073	65.154	65.755	70.236	68.207	68.260	70.132
13	44.784	43.532	43.326	46.168	36.903	34.991	34.776	37.851	66.572	64.927	64.716	65.278	71.480	70.088	69.892	71.811
14	44.777	44.222	43.660	47.815	37.035	35.867	35.289	39.930	63.404	62.397	61.846	63.075	71.262	70.432	69.930	72.079
15	43.846	44.058	43.037	47.001	36.907	36.216	35.516	40.291	58.003	57.401	56.738	57.857	68.218	67.739	67.145	68.307
16	41.867	40.893	41.371	44.134	36.568	34.377	35.445	39.437	50.724	48.743	49.668	50.126	61.449	59.838	60.564	59.754
17	38.608	37.384	38.281	38.521	36.039	33.723	35.002	36.953	42.111	39.975	41.137	40.025	49.910	48.087	49.070	44.802
18	33.573	32.354	32.275	32.096	35.049	32.458	32.942	33.785	33.311	30.866	31.298	31.300	32.599	30.333	30.693	28.708
19	30.518	29.122	28.585	28.486	33.905	31.549	31.300	31.358	29.654	27.400	27.172	27.435	23.450	21.211	20.995	21.521
20	29.755	28.254	27.609	27.205	33.113	30.752	30.235	30.026	28.903	26.646	26.175	26.162	22.712	20.480	20.034	20.261
21	28.977	27.640	26.965	26.301	32.285	30.077	29.497	29.022	28.105	26.008	25.472	25.186	21.924	19.827	19.347	19.282
22	28.370	27.153	26.307	25.656	31.643	29.514	28.750	28.239	27.495	25.465	24.759	24.497	21.325	19.302	18.630	18.583
23	27.677	26.639	25.754	25.098	30.937	28.928	28.122	27.588	26.822	24.902	24.157	23.814	20.638	18.740	18.045	17.908

Fig. 11. Mapping of heat distribution for streets with different height width ratio in correlation with average values of Universal Thermal Climate Index, Air Temperature, Surface Temperature, and Mean Radiant Temperature during summers

summer respectively. It was observed that with decreasing H/W ratio, air temperature increases. The difference in air temperature values is low during early morning hours (0500 hours - 1000 hours) in winter and (0500 hours - 0800 hours) in summers and during evening hours from (1800 hours - 0400 hours) in winters and (2000 hours and 0400 hours) in summers for all the cases. The temperature reaches its peak during noon hours in both seasons. The highest average air temperature value occurs at 1500 hours for a height to width ratio of 0.9 (40.29 °C in summers and 26.2°C in winters).

In winters, the temperatures begin to decline from 1700 hours in winters and 1900 hours in summers. It is noticed that the cooling rate in the wide street canyon isfaster than the narrow streets with a high height to width ratio. A difference of an average of 4 °C is also observed in surface temperature between streets where concrete is used as a major building material and streets where traditional building material (stone) and traditional construction techniques are applied. A similar trend is observed for mean radiant temperature in wide streets compared to narrow streets. The mean radiant temperature in a narrow street with an H/W ratio is recorded due to the thermal mass of the construction material and a less open area to release the heat. A comparative analysis of heat distribution for streets of different height-width ratios through average values of Air Temperature, Surface Temperature, Mean Radiant Temperature and Universal Thermal Climate Index for both winter and summer is shown in Fig. 10 and Fig. 11.

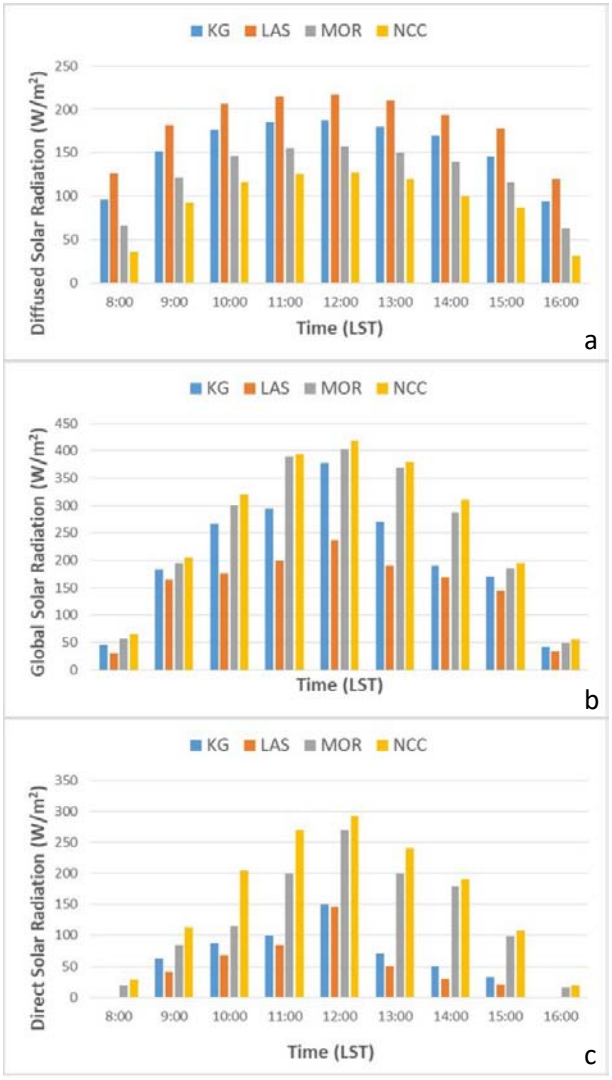

Figs. 11(a-c). (a) Diffused Solar Radiation, (b) Global Solara Radiation and (c) Direct Solar Radiation for four streets during winters

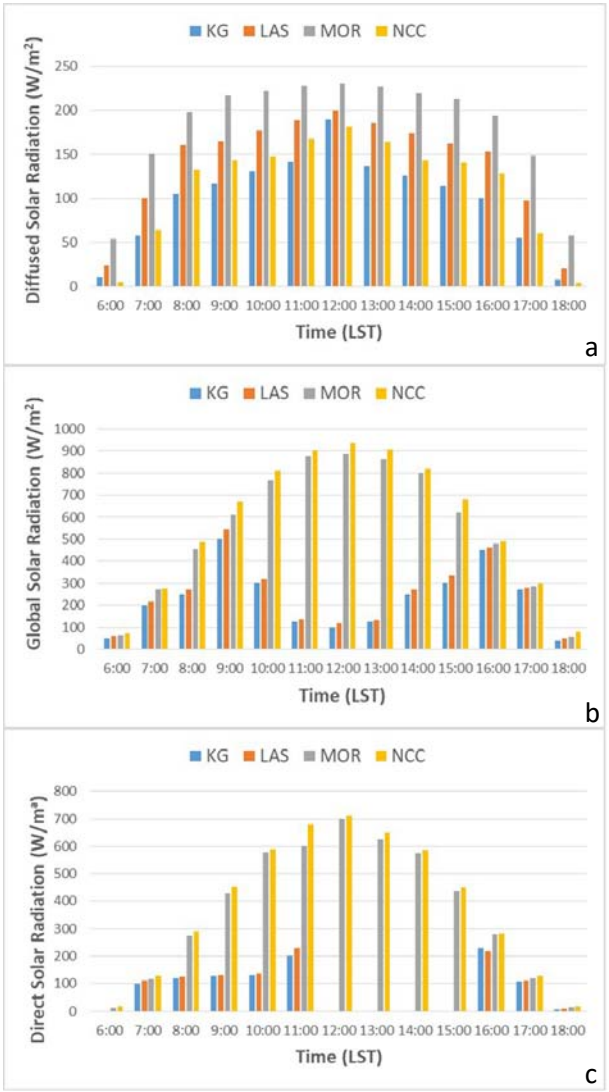

Figs. 12(a-c). (a) Diffused Solar Radiation, (b) Global Solara Radiation and (c) Direct Solar Radiation for four streets during summers

The short wave radiation fluxes are shown in Figs. 12 and 13 for winter and summer. The streets are warmer in summer as the aspect ratio decreases, but this trend is more prominent in E-W orientation streets (H/W = 1.6) due to high direct solar radiation. Global solar radiation is highly influenced by Direct solar radiation; hence similarities between the two solar components for streets can be observed in graphs [Figs. 11(b&c) and Figs. 12(b&c)]. In contrast, the Diffused solar radiation escalates with an increase in aspect ratio. This is due to the high amount of reflected radiation as the vertical surface area is more in such streets (H/W= 3.3 & 4.8). But the diffused radiation fluxes do not exceed 231 W/m^2 for all the streets and is noted to be maximum at 181 W/m^2 for the lowest height to width ratio street inthe SW-NE direction.

In other cases, the streets with a height to width ratio of 0.9 and 1.6 are highly exposed from 0900 hours to 1500 hours, with global radiation reaching a maximum of 903 W/m^2 in summers and 419 W/m^2 in winters. Despite the high H/W ratio, the east-west oriented street experiences a high heat gradient as the sun rays fall on the street laterally from both sides during the day. The NW - SE and N - S oriented streets with high H/W ratios (3.3 and 4.8, respectively) observe no direct solar exposure during peak heating hours (1200 hours to 1500 hours) in the streets in summers. As the height to width ratio increases, the time span of heat gain decreases in summers. Inversely high H/W ratio of streets does not support heat gain in winters; however, these streets (Kila Gate and Lashkar) have been shown to be thermally

comfortable due to the building materials and compact built form (XrYrZr and XrYrZu, respectively).

4. Conclusion

Outdoor thermal comfort was analysed in this study, using artificial neural network models. The Universal Thermal Climate Index was considered for evaluation as a measure of outdoor thermal comfort in four different streets. These streets represent four major zones of Gwalior city featuring composite climatic conditions. In order to develop ANN models, a funnel research approach was applied. First, using Pearson's correlation coefficient a linear relationship between input variables was determined. It was found that the mean radiant temperature is in high correlation with globe temperature and surface temperature. Based on the acquired results, meanradiant temperature was considered to be used in further analysis to avoid future redundancies and over-fitting concerns. Second, the ANFIS models were developed and processed to evaluate the impact of meteorological parameters on UTCI. Air temperature followed by mean radiant temperature, relative humidity and wind speed was found to have maximum impact on UTCI values for both summer and winters. This resonates with the previous findings found in literature. Therefore, two types of ANN Models were developed. One model used all the influencing meteorological parameters - air temperature, relative humidity, wind speed and the other used only air temperature. This study established that only air temperature can be used to predict outdoor thermal comfort using artificial neural networks. The validity of these models is evaluated through various statistical indices like coefficient of correlation, true predicted rate, false alarm rate and success index. R^2 in the summer season is found to be 0.852, 0.986, 0.962, 0.955 and in the winter season 0.976, 0.870, 0.941, 0.950 for Kila Gate (KG), Lashkar (LAS), Morar (MOR) and New City Centre (NCC) respectively. This highlights the efficiency of developed artificial neural network models. Similarly, the success index computed is in range 0.73 - 1 (Kila Gate), 0.88 - 1 (Lashkar), 0.86 - 1 (Morar), 0.87 - 1 (New City Centre) for the summer season and 0.78 - 0.99 (Kila Gate), 0.61 - 0.98 (Lashkar), 0.55 - 0.98 (Morar), 0.87 - 0.99 (New City Centre) for the winter season. These results conclude the high predictive ability of the developed artificial neural network model for both summer and winter seasons in composite climate. Nonetheless, the study also has its limitations in regard to data collection. The data set for the winter season is smaller than that for the summer season, owing to long summers in Gwalior city due to its location in a sub-tropical zone.The study contributes to smart city initiatives for future urban design and city planning for different urban microclimates to attain outdoor thermal comfort for reduced urban heat island and physical well-being to create sustainable cities and societies.

Acknowledgement

The authors thank the anonymous reviewers for their helpful suggestions and review which has led to substantial refinement in the original manuscript.The research was supported by All India Council for Technical Education, Government of India under its Research Promotion Scheme [File No. 8-207/RIFD/RPS (POLICY-1)/2018-19]. The first author was supported by the National Doctoral Fellowship Scheme under All India Council for Technical Education, Government of India.

Disclaimer : The contents and views expressed in this study are the views of the authors and do not necessarily reflect the views of the organizations they belong to.

References

Ali S. B. and Patnaik S, 2018, "Thermal comfort in urban open spaces: Objective assessment and subjective perception study in tropical city of Bhopal, India", *Urban Clim.*, **24**, 954-967, https://doi.org/10.1016/j.uclim.2017.11.006.

Amirtham, L. R., 2007, "Impact of built environment on outdoor thermal conditions in the hot humid city of Chennai, in: Conference on Sustainable Building South East Asia", Malaysia, 5-7.

ASHRAE & American National Standards Institute, 2004, "Thermal environmental conditions for human occupancy", 54th ed. American Society of Heating, Refrigerating and Air-Conditioning Engineers., Atlanta.

Banerjee, S., Middel, A. and Chattopadhyay, S., 2020, "Outdoor thermal comfort in various microentrepreneurial settings in hot humid tropical Kolkata: Human biometeorological assessment of objective and subjective parameters", *Sci. Total Environ*., 137741. https://doi.org/10.1016/j.scitotenv.2020.137741.

Basha, G., Kishore, P., Ratnam, M. V., Jayaraman, A., Kouchak, Amir Agha Ouarda, Taha B. M. J. and Velicogna, I., 2017, "Historical and Projected Surface Temperature over India during the 20th and 21st century", *Sci. Rep.* **7**, 1-10, https://doi.org/10.1038/s41598-017-02130-3.

Binte, S. and Patnaik, S., 2017, "Urban Climate Thermal comfort in urban open spaces Objective assessment and subjective perception study in tropical city of Bhopal", India. *Urban Clim*., 0-1. https://doi.org/10.1016/j.uclim.2017.11.006.

Bozorgi, M. and Nejadkoorki, F., 2018, "Land surface temperature estimating in urbanized landscapes using artificial neural networks", *Environ. Monit. Assess*. https://doi.org/doi.org/10.1007/s10661-018-6618-2

Bureau of Indian Standards, 2016. National Building Code.

Census of India 2011, 2020, "Population Projections for India and States 2011 - 2036", National Commission on Population Ministry of Health & Family Welfare, Nirman Bhawan, New Delhi.

Chan, S. Y. and Chau, C. K., 2019, "Development of artificial neural network models for predicting thermal comfort evaluation in urban parks in summer and winter", *Build. Environ*., **164**, 106364. https://doi.org/10.1016/j.buildenv.2019.106364.

Cheng, V., Steemers, K., Montavon, M. and Compagnon, R., 2006, Urban Form , Density and Solar Potential.

Chronopoulos, K., Kamoutsis, A., Matsoukis, A. and Manoli, E., 2012, "An artificial neural network model application for the estimation of thermal comfort conditions in mountainous regions, Greece", *Atmósfera*, **25**, 2, 171-181.

Das M, Das A, Mandal S, 2020, "Outdoor thermal comfort in different settings of a tropical planning region: A study on Sriniketan-Santiniketan Planning Area (SSPA), Eastern India", *Sustain. CitiesSoc*., **63**, 102433. https://doi.org/10.1016/j.scs.2020.102433

Dombaycı, O. A. and Golcu, M., 2009, "Daily means ambient temperature prediction using artificial neural network method A case study of Turkey", *Renew. Energy*, **34**, 1158-1161. https://doi.org/10.1016/j.renene.2008.07.007.

Gobakis, K., Kolokotsa, D., Synnefa, A., Saliari, M., Giannopoulou, K. and Santamouris, M., 2011, "Development of a model for urban heat island prediction using neural network techniques", *Sustain. Cities Soc*., **1**, 104-115. https://doi.org/10.1016/j.scs.2011.05.001.

Horrison, E. and Amirtham, L. R., 2016, "Role of Built Environment on Factors Affecting Outdoor Thermal Comfort - A Case of T. Nagar, Chennai", India **9**, 3-6. https://doi.org/10.17485/ijst/2016/v9i5/87253.

Horrison, E., Rajan, S. and Rose, L., 2021, "Urban heat island intensity and evaluation of outdoor thermal comfort in Chennai, India". *Environ. Dev. Sustain*. https://doi.org/10.1007/s10668-021-01344-w.

Ivana, S. Bogdanovic, P., Vukadinovic, A. V., Jasmina M. Radosavljevic, M. A. and Mitkovic, M. P., 2016, "Forecasting of Outdoor Thermal Comfort Index in Urban Open Spces : The Nis Fortress Case Study", *Therm. Sci*., **20**, 1531-1540. https://doi.org/10.2298/TSCI16S5531B.

Ketterer, C. and Matzarakis, A., 2016, "Mapping the Physiologically Equivalent Temperature in urban areas using artificial neural network", *Landsc. Urban Plan*., **150**, 1-9. https://doi.org/10.1016/j.landurbplan.2016.02.010.

Kotharkar, R., Bagade, A. and Agrawal, A., 2019, "Investigating Local Climate Zones for Outdoor Thermal Comfort Assessment in an Indian City", *Geogr. Pannonica*, **23**, 318-328. https://doi.org/10.5937/gp23-24251.

Krzysztof Błażejczyk, n.d. BioKlima [WWW Document]. Dep. Geoecology Climatol. Inst. Geogr. Spat. Organ. Polish Acad. Sci. URL https://www.igipz.pan.pl/bioklima.html.

Lee, Y. Y., Kim, J. T. and Yun, G. Y., 2016, "The neural network predictive model for heat island intensity in Seoul. Energy Build", **110**, 353-361. https://doi.org/10.1016/j.enbuild.2015.11.013.

Manavvi, S.and Rajasekar, E., 2021, "Evaluating outdoor thermal comfort in "Haats" - The open air markets in a humid subtropical region", *Build. Environ*., **190**, 107527. https://doi.org/10.1016/j.buildenv.2020.107527.

Manavvi, S.and Rajasekar, E., 2019, "Semantics of outdoor thermal comfort in religious squares of composite climate: New Delhi", India, *International Journal of Biometeorology*, **64**, 1. doi : 10.1007/s00484-019-01708-y.

Mehrotra, S., Subramanian, D., Bardhan, R. and Jana, A., 2021, "Urban Climate Effect of surface treatment and built form on thermal profile of open spaces : A case of Mumbai", India, *Urban Clim*., **35**, 100736. https://doi.org/10.1016/j.uclim.2020.100736.

Milojevic-Dupont, N. and Creutzig, F., 2021, "Machine learning for geographically differentiated climate change mitigation in urban areas", *Sustain. Cities Soc*., **64**, 102526. https://doi.org/10.1016/j.scs.2020.102526

Mohan, M., Sati, A. P. and Bhati, S., 2020, "Urban Climate Urban sprawl during five decadal period over National Capital Region of India: Impact on urban heat island and thermal comfort ", *Urban Clim.*, **33**, 100647. https://doi.org/10.1016/j.uclim.2020.100647.

Moustris, K., Tsiros, I. X., Tseliou, A. and Nastos, P., 2018, "Development and application of artificial neural network models to estimate values of a complex human thermal comfort index associated with urban heat and cool island patterns using air temperature data from a standard meteorological station", *Int. J. Biometeorol*. https://doi.org/https://doi.org/10.1007/s00484-018-1531-5.

Moustris, K. P., Nastos, P. T. and Paliatsos, A. G., 2013, "One-Day Prediction of Biometeorological Conditions in a Mediterranean Urban Environment Using Artificial Neural Networks Modeling", *Adv. Meteorol*., 2013. https://doi.org/http://dx.doi.org/10.1155/2013/538508 Research.

Nutkiewicz, A., Jain, R. K. and Bardhan, R., 2018, "Energy modeling of urban informal settlement redevelopmentExploring design parameters for optimal thermal comfort in Dharavi, Mumbai", India. *Appl. Energy*, **231**, 433-445. https://doi.org/10.1016/j.apenergy.2018.09.002.

Papantoniou, S. and Kolokotsa, D., 2015, "Prediction of outdoor air temperature using Neural Networks; application in 4 European cities", *Energy Build*. https://doi.org/10.1016/j.enbuild.2015.06.054.

Protic, Ivana Bogdanovic, Vukadinovic, Ana, Radosavljevic, Jasmina and Alizamirc, Meysam, 2016, "Forecasting of outdoor thermal comfort index in urban open spaces the nis fortress case study", *Thermal Science*, 1531-1539.

Sharma, R., Pradhan, L., Kumari, M. and Bhattacharya, P., 2021, "Urban Climate Assessing urban heat islands and thermal comfort in Noida City using geospatial technology", *Urban Clim.*, **35**, 100751. https://doi.org/10.1016/j.uclim.2020.100751.

Silva, J. P., 2017, "Solar radiation and street temperature as function of street orientation", An analysis of the status quo and simulation of future scenarios towards sustainability in Bahrain. E3S Web Conf. 23. https://doi.org/10.1051/e3sconf/20172302002.

Silva, J. P., 2021, "Streets are forever: thermal coefficient of street orientation as a strategy to develop cooler street networks in hot climates", *Archit Sci Rev*., **64**, 225-34. https://doi.org/10.1080/00038628.2019.1703637**.**

United Nations, 2017, Global status report 2017.

UTCI, 2021, Universal Thermal Climate Index [WWW Document]. URL http://www.utci.org/

Vouterakos, P. A., Moustris, K. P., Bartzokas, A., Ziomas, I. C., Nastos, P. T. and Paliatsos, A. G., 2012, "Forecasting the discomfort levels within the greater Athens area, Greece using artificial neural networks and multiple criteria analysis", *Theor. Appl. Climatol*., **110**, 329-343. https://doi.org/10.1007/s00704-012-0626-x.

Vučković, D., Jovic, S., Bozovic, R., Džamićc, V. and Kićovićd, D., 2019, "Urban Climate Potential of neuro-fuzzy methodology for forecasting of outdoor thermal comfort index at urban open spaces", *Urban Clim*., **28**. https://doi.org/10.1016/j.uclim.2019.100467.

Weerasuriya, A. U., Zhang, X., Lu, B., Tse, K. T. and Liu, C., 2020, "Optimizing Lift-up Design to Maximize Pedestrian Wind and Thermal Comfort in 'Hot-Calm' and 'Cold-Windy' Climates", *Sustain. Cities Soc*., **58**, 102146. https://doi.org/10.1016/j.scs.2020.102146.

Ziaul, S. and Pal, S., 2019, "Assessing outdoor thermal comfort of English Bazar Municipality and its Surrounding, West Bengal", India. *Adv. Sp. Res*. https://doi.org/10.1016/j.asr.2019.05.001.

Appendix 1

```
import pandas as pd

df = pd.read_csv('TPR, FAR , SI_summers.csv')
# O_PET = df.iloc[:, 0]
# P_PET = df.iloc[:, 1]
O_UTCI = df.iloc[:, 1]
P_UTCI = df.iloc[:, 2]

O_UTCI = list(O_UTCI)
P_UTCI = list(P_UTCI)

lim = [[-2000, -40], [-40, -27], [-27, -13], [-13, 0], [0, 9], [9, 26], [26, 32], [32, 38], [38, 46], [46, 2000]]

n = len(O_UTCI)

for l, u in lim:
    X = 0
    Y = 0
    Z = 0
    for i in range(n):
        if l < O_UTCI[i] <= u and l < P_UTCI[i] <= u:
            X += 1
    for i in range(n):
        if l < O_UTCI[i] <= u:
            if P_UTCI[i] > u or P_UTCI[i] <= l:
                Y += 1
    for i in range(n):
        if l < P_UTCI[i] <= u:
            if O_UTCI[i] > u or O_UTCI[i] <= l:
                Z += 1

    W = n - (X + Y + Z)

    print('X - ', X)
    print('Y - ', Y)
    print('Z - ', Z)
    print('W - ', W)

    try:
        TPR = X / (X + Y)
    except Exception as e:
        print(e, '1')
        TPR = '-'

    try:
        FAR = Z / (Z + X)
    except Exception as e:
        print(e, '2')
        FAR = '-'

    try:
        SI = (X + W) / (X + Y + Z + W)
    except Exception as e:
        print(e, '3')
        SI = '-'

    print('TPR - ', TPR)
    print('FAR - ', FAR)
    print('SI - ', SI)

    print(l, u)
```